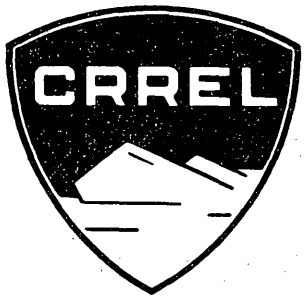

Research Report 193

LIGHT SCATTERING AND PARTICLE AGGREGATION IN SNOWSTORMS

by

Malcolm Mellor

FEBRUARY 1966

U.S. ARMY MATERIEL COMMAND
COLD REGIONS RESEARCH & ENGINEERING LABORATORY
HANOVER, NEW HAMPSHIRE

DA Task 1VO25001A13001

PREFACE

This report describes preliminary studies on optical scattering by falling snow. The work was carried out by Mr. Malcolm Mellor, Experimental Engineering Division (Mr. K. A. Linell, Chief). The author is grateful to Dr. Andrew Assur, Scientific Advisor, USA CRREL for drawing attention to the problem and for encouraging the work described here. He is also indebted to Dr. Uwe Radok and Mr. William Budd for a review of the manuscript.

USA CRREL is an Army Materiel Command laboratory.

DA Project IV025001A13001

CONTENTS

	Page
Preface	ii
Summary	iv
Introduction	1
Light scattering and brightness contrast	1
Measurements of visibility and brightness contrast	2
Attenuation as a function of density	3
Concentration and aggregation of falling snow particles	5
Presentation of light attenuation data	8
Literature cited	10
Appendix A: Visual range data	11
Appendix B: Particle concentration	15
Appendix C: Estimated particle mass	16

ILLUSTRATIONS

Figure

1. Extinction coefficient and visual range related to the $\frac{1}{3}$ density of suspended snow ---- 4
2. $N^{\frac{1}{3}}$ plotted against snow density ---- 5
3. Mean mass of single snow particles plotted against snow density ---- 6
4. Concentration of discrete particles at ground level ---- 7
5. Histogram giving frequency distribution for snow particle and snowflake fall velocity ---- 9
6. Extinction coefficient and visual range related to snow accumulation rate for snow falling in wind-free conditions ---- 9

SUMMARY

Attenuation of visible radiation by falling snow was studied by a method based on brightness contrast between topographic features and the adjacent sky. Extinction coefficient and visual range are related to snow density, and are compared with data for Antarctic blizzards. Since attenuation depends more on the size and concentration of discrete particles than on the mass density of suspended snow, the process of particle aggregation and snowflake formation during fall is considered by collision theory, and an expression describing aggregation effects is developed. This offers an explanation for the relative constancy of particle concentration observed at ground level during snowfalls of varying intensity. Since there is no strong justification for relating extinction coefficient to snow density, an empirical correlation between extinction coefficient and precipitation rate is given for practical use. It is shown that visual range estimated by eye in hilly terrain may be less than the true value, since sky brightness is locally reduced over broad hilltops with low albedo.

LIGHT SCATTERING AND PARTICLE AGGREGATION IN SNOWSTORMS

by

Malcolm Mellor

Introduction

When practical questions concerning attenuation of visible radiation by falling snow were raised, cursory search of the literature revealed little relevant information. In view of the complex shape of snow particles a purely theoretical approach seemed undesirable, and so an immediate attempt was made to measure the attenuation of light transmitted through falling snow from a diffuse source. This proved unsatisfactory, since the photometric device available at that time was insufficiently sensitive for work over the necessarily short (~100 m) transmission path. Interim working estimates of extinction coefficient were therefore made from visibility data for Antarctic blizzards, supplied prior to publication by Radok (see Budd, Dingle and Radok, 1965).

During the remainder of the winter (1964-1965) simple measurements of visual range were made for a variety of conditions experienced at Hanover, N. H., and some control measurements were made with a telephotometer. These data have provided information on light attenuation by falling snow, and have also given rise to some interesting speculations regarding particle aggregation during snowfall.

Light scattering and brightness contrast

As an alternative to measuring beam attenuation directly, extinction coefficients for falling snow may be determined by considering the reduction of brightness contrast between a dark target and the adjacent horizon sky. Relevant theory, originated by Koschmieder and reviewed by Middleton (1952), Johnson (1954) and others, is outlined below.

Consider a cone of vision directed horizontally through a uniform field of snow-filled air. The cone is illuminated uniformly, say by sunlight diffused through a dense overcast. Snow particles in a representative elementary volume of the cone scatter light (independently and incoherently), so that the element has a brightness, or luminance, B_h which is determined by the incident illumination and by the number and nature of the snow particles. B_h is the intrinsic brightness of the snow-filled element, but the apparent brightness sensed by an observer at the apex of the cone of vision is reduced by scattering in the intervening snow cloud. In the cone, luminous flux and brightness do not change with distance from the apex x if the air is perfectly clear; brightness B diminishes with x only because of scattering from snow particles, and attenuation follows the Bouger-Lambert law:

$$\frac{dB}{B} = -\sigma\, dx \qquad (1)$$

where σ is the extinction coefficient or, since absorption is probably negligible for snow, the scattering coefficient. It is assumed independent of x. In general σ is a function of wavelength, but since snow particles are very large compared with the wavelength of visible radiation it is expected to be almost independent of wavelength in the visible range. Solution of eq 1 with the condition $B = B_h$ when $x = 0$ yields a substitution for B in eq 1:

$$B = B_h e^{-\sigma x}. \qquad (2)$$

When the line of sight is directed through an effectively infinite thickness of the snow cloud, i.e., towards the horizon sky, the total apparent brightness sensed by the observer B_{ah} is found by integrating throughout the cone between the limits

$x = 0$ and $x = \infty$:

$$B_{ah} = B_h \sigma \int_0^{\infty} e^{-\sigma x} dx = B_h. \tag{3}$$

When the line of sight is directed instead to a "black" target of zero luminance, horizontal distance X from the observer, the total apparent brightness sensed by the observer B_{at} is:

$$B_{at} = B_h \sigma \int_0^{X} e^{-\sigma x} dx = B_h (1 - e^{-\sigma X}). \tag{4}$$

If the target is not black but has an intrinsic brightness B_0, the apparent brightness sensed by the observer B_{at}' is the brightness of the limited cone B_{at} plus the attenuated brightness of the target itself:

$$B_{at}' = B_h (1 - e^{-\sigma X}) + B_0 e^{-\sigma X}. \tag{5}$$

The apparent contrast C between a distant target of sufficient size and the horizon sky is:

$$C = \frac{B_{at}' - B_h}{B_h}. \tag{6}$$

The intrinsic contrast C_0 between the target and the adjacent horizon sky as $X \rightarrow 0$ is:

$$C_0 = \frac{B_0 - B_h}{B_h}. \tag{7}$$

C_0 may take values from -1 for a black body up to positive values for self-luminous targets. Equation 5 can now be rewritten in terms of brightness contrast:

$$C = C_0 e^{-\sigma X} \tag{8}$$

or

$$\sigma = \frac{1}{X} \ln\left(\frac{C_0}{C}\right). \tag{9}$$

If we define a visual range V as the distance X between observer and target at which apparent contrast C diminishes to the minimum level distinguishable by eye (termed the liminal contrast ϵ), then eq 9 becomes a relation between extinction coefficient and visual range. It has been found that under a wide range of daylight conditions the average human eye can discern a target of adequate size (say greater than 1° visual angle) if the apparent contrast exceeds 2%. From this there follows a standard definition of the meteorological visual range V_m as the maximum distance at which the average eye can distinguish a black target of suitable size, i.e., with $C_0 = -1$ and $\epsilon = -0.02$,

$$V_m = \frac{3.912}{\sigma}. \tag{10}$$

Measurements of visibility and brightness contrast

Simultaneous measurements of visual range and snow density were made on all occasions when conditions were judged to be suitable according to the following criteria: (1) sky completely overcast, (2) little or no wind, (3) snow density steady with time and distance for the duration of an observation (snow squalls were not

sampled). Visual range was estimated by using as targets a succession of pine-covered hills and ridges, all of similar height to the observation point. The vertical mass flux of snow was measured by exposing a tray for a timed interval and weighing the catch. The mean vertical component of snow particle velocity was measured by timing the fall of particles through a vertical distance of approximately 3 m at several different locations. With some care and practice this measurement could be made consistently simply by following particles, or groups of particles, by eye and timing their fall with a stop-watch. Snow density was obtained by dividing the vertical mass flux by the fall velocity.

In the latter part of the study period attempts were made to measure number density as well as mass density. When falls were predominantly of simple single particles the number flux could be obtained by exposing a cooled tray for a brief timed period (about 10 sec) and then counting the particles seen through 10 windows of a template laid over the tray. Snowflakes and other fragile aggregations of particles usually shattered into their components on hitting the tray, but late in the study it was found that the required flux estimates could be made by exposing a warmed tray for about 5 sec and counting the water marks. The simultaneous measurements of mass flux and number flux for single particle falls yielded estimates of mean particle mass for various types of snow crystals.

Photometric control readings were made with a Spectra brightness meter, model UB $1\frac{1}{2}$, with stabilized power source and external galvanometer. The meter accepts light from a $1\frac{1}{2}°$ solid angle. Target brightness was compared with the brightness of adjacent horizon sky for several targets lying at distances of 15 m to 3.1 km. Readings were made using a filter which simulates the spectral response of the human eye, and also with blue ($\approx$0.445μ) and red ($\approx$0.585μ) filters. Extinction coefficient was obtained graphically in accordance with eq 9. Results of observations are tabulated in Appendixes A, B and C.

Attenuation as a function of density

This work was originally intended to determine extinction coefficient for falling snow and to relate it to some descriptive index such as snow density or precipitation rate. Before proceeding to this end result, however, it seems desirable to inquire into the justification for such relationships.

Results from standard electromagnetic theory provide a relation which expresses the scattering coefficient for spherical aerosols as the total effective scattering area per unit volume:

$$\sigma = KNa \qquad (11)$$

where N is the number of particles per unit volume, $\underline{a}$ is the cross-sectional area of a particle normal to the beam, and K is the scattering area ratio, i.e., the area of wave front affected by a particle divided by the actual particle area $\underline{a}$. (Strictly speaking, particle size distribution should be taken into account by writing the summation $\sigma = \sum_{i=1}^{n} K_i N_i a_i$, but here we seek simplicity.)

The numerical concentration of particles N in falling or blowing snow is not easy to measure, but the mass density γ can be obtained without too much trouble. It is therefore convenient to express N as a function of γ, at least for simple particle shapes:

$$N = \frac{A_1}{\ell^3} \frac{\gamma}{\gamma_i} \qquad (12)$$

where ℓ is a characteristic linear dimension of the particle, γ_i is ice particle density, and A_1 is a dimensionless constant. The particle cross section $\underline{a}$ is proportional to ℓ^2, so that eq 11 can be rewritten as:

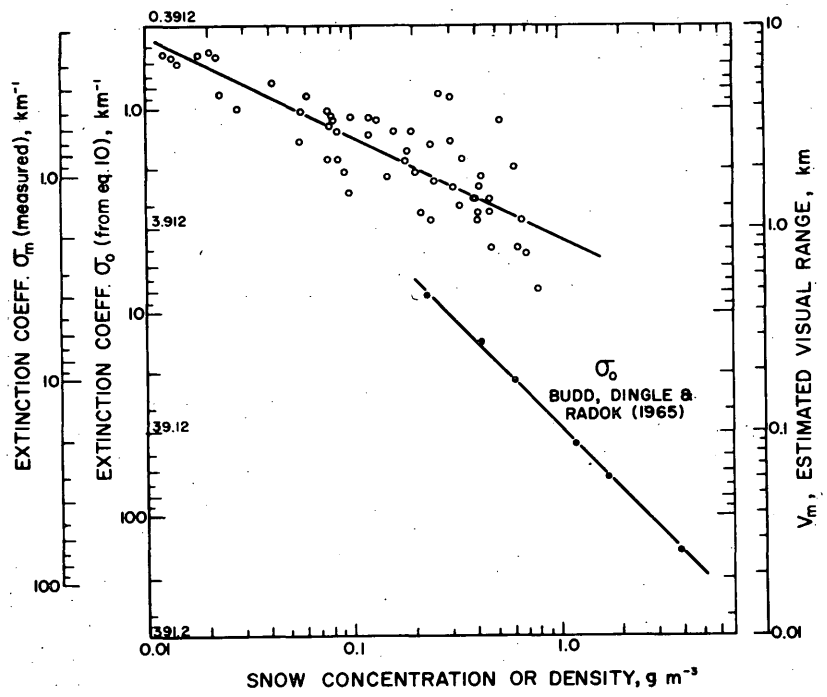

Figure 1. Extinction coefficient and visual range related to the density of suspended snow. Note that a direct comparison of σ_0 for the Antarctic blizzard with σ_m for falling snow brings the data into coincidence for the mid-range of densities.

$$\sigma = \frac{A_2 K_\ell}{\ell} \cdot \frac{\gamma}{\gamma_i} \qquad (13)$$

where A_2 is constant for a given shape of particle and K_ℓ is a function of particle size and shape, though perhaps a weak function in view of the large particle size for snow.

When snow is blown by strong winds the grains are usually equant and often rounded; the particle size and the size distribution at a height of 2 m or so apparently vary little from time to time and place to place. Under these circumstances A_2, K_ℓ, and ℓ are constants, and a linear relation between σ and γ is to be expected. Visibility data for Antarctic blizzards by Budd, Dingle and Radok (1965) show that this is indeed the case (Fig. 1), and therefore it is entirely logical to express σ as a function of γ for blowing snow. Since Budd et al. give particle sizes it is possible to calculate the approximate value of K_ℓ. If it is assumed that the visibility estimates were in accordance with the meteorological standard,* i.e., $C_0 = -1$ and $\epsilon = 0.02$, values of K_ℓ between 1.8 and 2.7 are obtained, depending on how ℓ is defined for the non-spherical particles. These values may be compared with the limiting value of 2 given by Mie theory.

*This assumption is not strictly justifiable, since the stakes used for targets were neither black nor sufficiently wide. However, Liljequist's (1957) data for blizzard visibility as a function of wind speed indirectly support Dingle's measurements.

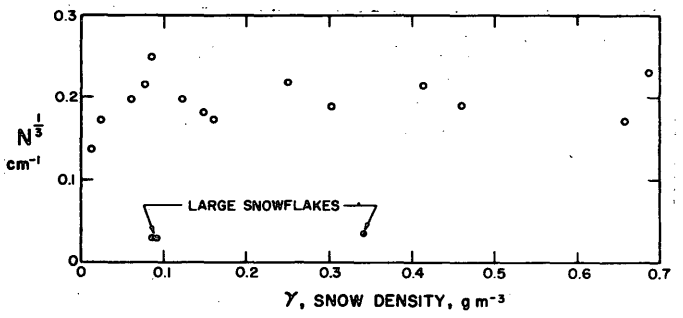

Figure 2. $N^{\frac{1}{3}}$ plotted against snow density.

When snow is falling in relatively calm weather the size and shape of crystals and flakes vary widely with atmospheric conditions, and it would be surprising if σ remained simply related to γ. However, while $A_2 K_\ell / \ell$ is not likely to be constant, there could still be linear correlation between σ and γ if $A_2 K_\ell / \ell$ does not vary systematically with γ. The data of Figure 1 dispel this possibility; any relation between σ and γ is clearly non-linear. A first guess from the logarithmic plot is that σ might be proportional to γ^n, where $n < \frac{2}{3}$.

The difficulty at this point is that there is no prima facie evidence for a simple relation between γ and the total scattering area Na. It becomes necessary to consider how particle size and concentration vary for snowstorms generally.

Concentration and aggregation of falling snow particles

As a starting point for this discussion, we explore the implications of the power relation between σ and γ mentioned above. The most clearly defined limit of the data in Figure 1 gives a maximum value of the exponent $n \approx \frac{2}{3}$, and if eq 13 is appropriately rearranged we see that this value implies that $N^{\frac{1}{3}}$ is constant, or at least does not vary appreciably with γ. In Figure 2 $N^{\frac{1}{3}}$ is plotted against γ, and it can be seen that overall there is no significant correlation. With the exception of one set of observations the values of $N^{\frac{1}{3}}$ vary little over the observed range of conditions. Since $N^{\frac{1}{3}}$ is a relatively weak function there is greater variation in the values of N, but nevertheless it seems legitimate to consider whether N is kept within certain limits by some mechanism.

First of all, it may be recalled that nucleation of ice crystals from supercooled cloud droplets usually requires freezing nuclei, which are typically kaolinite particles from terrestrial dust. In some geographical locations the concentration of freezing nuclei may be fairly constant over the winter period, although the efficiency of nucleation apparently depends to some extent on temperature. If N were held between fairly narrow limits by availability of freezing nuclei, then the density of falling snow would be determined by the mass of the individual particles. Crystal form and size depend on temperature and degree of supersaturation of the atmosphere, and in general there is a correlation between air temperature at an observation station and the size of snow crystals encountered there. Intensity of snowfall also tends to be related to air temperature, but it is not known whether there is a correlation between particle size and intensity of snowfall. Using the very rough data from the present observations, and checking estimated crystal masses against Mason's (1962) data for generally larger crystals, particle mass has been plotted against snow density in Figure 3. There is little apparent correlation, although a systematic trend might still be found with more precise data and wider sampling. Group averages of the data suggest a slight increase of particle mass as density increases.

So far no mention has been made of particle aggregation, although light scattering depends on the concentration of discrete particles rather than the absolute number of crystals present. Winters at Hanover are cold, and heavy snowfall with large flakes is quite rare, but on one occasion when large snowflakes fell with temperatures near the freezing point the concentration of flakes was relatively low—about two orders

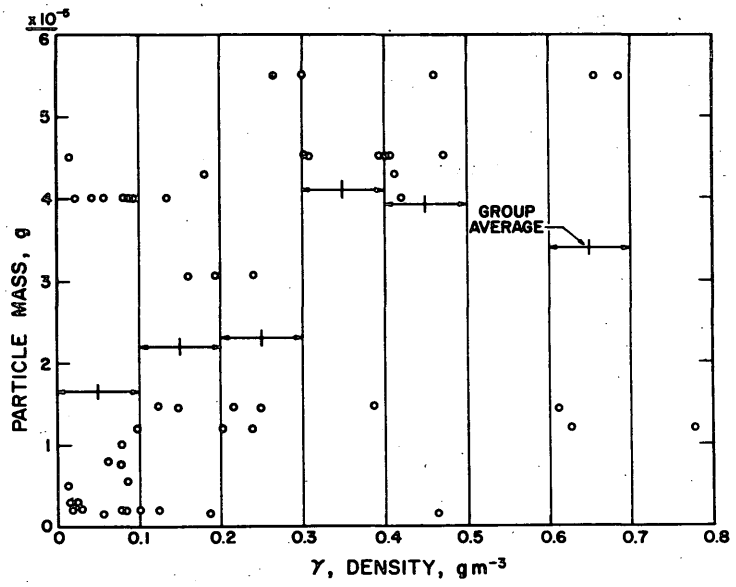

Figure 3. Mean mass of single snow particles plotted against snow density.

of magnitude smaller than typical concentrations for snowfall in cold weather. Visual range on this occasion was abnormally great for snow of that density. We should therefore give some thought to the collision process by which flakes and other aggregations are formed.

Consider a large unit volume which encloses many falling particles and which moves downward at the mean fall velocity of the enclosed particles. In general, neighboring particles move relative to each other; size, shape, and hence fall velocity, of individual particles vary, and aerodynamic instability of planar crystals causes "fluttering" oscillations. Free air turbulence is probably unimportant, as it tends to produce in-phase displacement over relatively large volumes. A mean free path for the particles $\overline{L}$ may be defined as:

$$\overline{L} = \frac{1}{N \overline{a}_c} \tag{14}$$

where $\overline{a}_c$ is a mean "collision cross section" for the particles. This will probably correspond closely to the geometric cross section, although it could be defined to accommodate the effects of any net electrostatic attractions.

We introduce a "wandering velocity" $\overline{v}$, which is the deviation from the mean fall velocity of all the particles, determined largely by the shape and size distribution of the particles. The frequency of collision for a particle f is therefore:

$$f = \frac{\overline{v}}{\overline{L}} . \tag{15}$$

When two particles collide they may simply rebound, or they may adhere to form a single larger particle. The probability of adhesion will be determined by the geometry of the colliding grains and by the physical state of their surfaces; intricate dendrites will readily interlock, and warm crystals with high specific surface or extreme local curvature will adhere tenaciously. To express the proportion of collisions which result in adhesion we introduce an "aggregation efficiency" E.

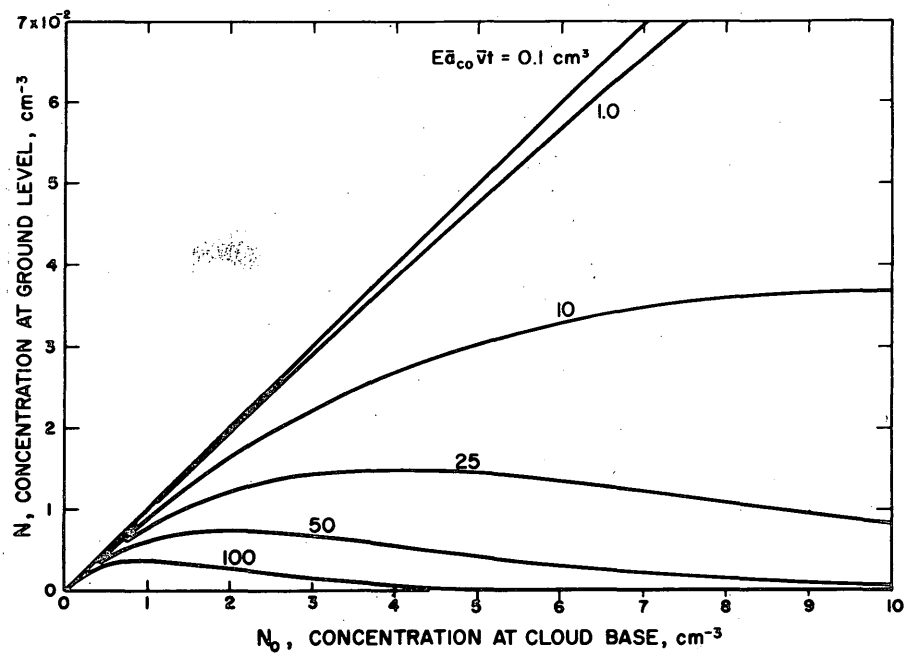

Figure 4. Concentration of discrete particles at ground level (N) as a function of particle concentration at the base of the parent cloud (N_0), according to eq 17.

It is now possible to write an expression for the rate at which particles are removed in effect from the cloud by collision and adhesion:

$$\frac{dN}{dt} = -EN\frac{\bar{v}}{\bar{L}} . \qquad (16)$$

$\bar{L}$ is actually a function of N, but we now assume that the collision cross section of two adhering particles is the sum of their individual cross sections and so, since $N\bar{a}_c$ is constant, $\bar{L}$ becomes constant for a given snowfall.

If particles fall from their parent cloud with initial concentration N_0 at time $t = 0$, the solution of eq 16 is:

$$N = N_0 \exp(-E\bar{v}t/\bar{L})$$

or (17)

$$N = N_0 \exp(-EN_0\,\bar{a}_{c0}\,\bar{v}t).$$

Hence the concentration of discrete particles N diminishes exponentially with time during fall and the rate constant for the decay depends on the size of individual particles, on the "wandering velocity," and on the aggregation efficiency.

An interesting aspect of eq 17 is the way in which N at ground level varies with initial concentration N_0 when other parameters are held constant; no matter how abundant the particles at the cloud base, in general the concentration at ground level is limited. This is illustrated in Figure 4 for a range of values of ($E\,\bar{a}_{c0}\,\bar{v}\,t$) chosen to conform with the following estimates of magnitudes: $E \sim 10^{-1}$ to 1, $\bar{a}_{c0} \sim 10^{-4}$ to

10^{-1} cm^2, $\bar{v}$~10 cm/sec, t~10^3 sec. On these assumptions there is virtually no aggregation of very small particles during a typical fall, but large stellar dendrites aggregate so fast that the concentration of resulting snowflakes at ground level can never be very high.

The midwinter snowfalls observed in Hanover typically had spatial dendrites of about 0.5 mm diameter, and assuming these to have an aggregation efficiency of about 0.8 the corresponding value of ($E \bar{a}_{c0} \bar{v} t$) is 20. For this condition Figure 4 shows only a slow change of N with N_0, and the appropriate curve traverses the range of observed values for N (5×10^{-3} to 15×10^{-3} cm^{-3}). Since mass density γ is a measure of N_0 for a given type of snow, we thus have a possible explanation for the apparent constancy of n with γ which prompted this discussion.

For the rare falls of large (5 mm) stellar dendrites mentioned above, the value of ($E \bar{a}_{c0} \bar{v} t$) is about 10^3 cm^{-3}. Although the curve for this value is unplottable on the scale of Figure 4, it gives the maximum concentration N after a fall of 10^3 sec of order 10^{-4} cm^{-3}, which may be compared with the observed snowflake concentrations of 2 to 4×10^{-5} cm^{-3}.

Presentation of light attenuation data

In view of the foregoing it seems unprofitable to fit an empirical regression line to the data of Figure 1. In fact, for practical purposes there seems to be no special merit in relating extinction coefficient to snow density if a wide range of snow types has to be accommodated. Since fall velocity does not vary greatly (Fig. 5) it is just as satisfactory, and much more convenient, to relate extinction coefficient to the more easily measurable precipitation rate. This procedure is, of course, only applicable when snow is falling in calm weather.

Figure 6 shows the correlation between visual range and snow accumulation rate and also between extinction coefficient and snow accumulation rate. The regression line yields the relations:

$$V_m = 0.625\, A^{-0.421} \qquad (18)$$

where V_m is in km and A, the snow accumulation rate, is in g cm^{-2} hr^{-1}

and $$\sigma_0 = 6.26\, A^{0.421} \qquad (19)$$

where σ_0, the extinction coefficient according to eq 10, is in km^{-1} and A is in g cm^{-2} hr^{-1}. The extinction measurements made photometrically show that σ_0 is actually about twice the true value for extinction coefficient; for the range of conditions checked by control measurements the true extinction coefficient σ_m follows the relation:

$$\sigma_m = 0.467\, \sigma_0 = 2.92\, A^{0.421} \text{ km}^{-1}. \qquad (20)$$

The exponent in eq 19 and 20 is approximately equal to $\frac{1}{2}$, but this does not appear to have any obvious dimensional significance.

It should be noted here that visual ranges and extinction coefficient become largely dependent on other factors, notably water vapor, when snowfall is very light.

The discrepancy between σ_0 and σ_m is apparently due mainly to a gradient of sky brightness above the hilltops used as targets. Contrast was measured between the target and the sky a few degrees of elevation above it, while the visual estimates depended on contrast between the target and the sky immediately adjacent to it. Measurements showed that sky brightness immediately above a hilltop was significantly lower than that a few degrees higher, probably because of the low albedo of the broad hilltop. This effect is roughly comparable to the "water sky" phenomenon known to polar navigators. A less important factor was the inherent contrast of the targets C_0; instead of the assumed value -1, C_0 was measured at values close to -0.9 for each of the three filters.

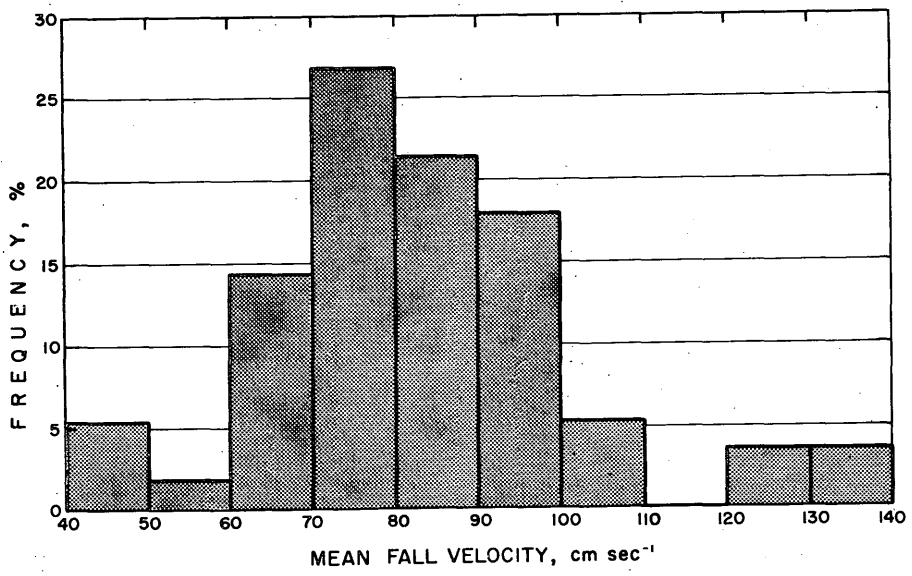

Figure 5. Histogram giving frequency distribution for snow particle and snowflake fall velocity (covering all observations made at Hanover, N. H., during winter of 1964/65).

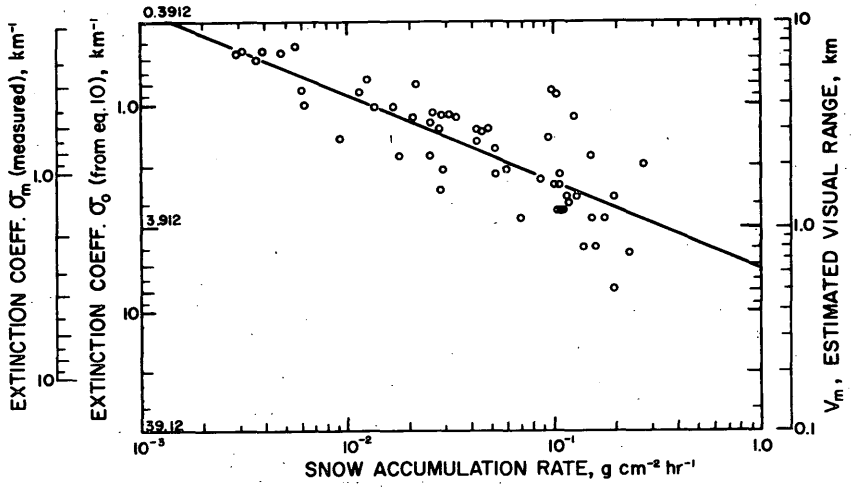

Figure 6. Extinction coefficient and visual range related to snow accumulation rate for snow falling in wind-free conditions.

Targets of small horizontal extent should not disturb the sky brightness, and therefore the values of σ_0 obtained from the data of Budd et al. are probably close to the true values. When corrected coefficients σ_m from this study are compared with the σ_0 values for the **Antarctic blizzard,** they are of the same magnitude in the range of snow densities common to both studies.

The simple photometric measurements gave no significant correlation between extinction and wavelength in the narrow range observed ($\approx 0.4\mu$-0.6μ).

LITERATURE CITED

Budd, W., Dingle, R. and Radok, U. (1965) "The Byrd snow drift project—outline and basic results" in Antarctic research series, vol. 7 (M. Rubin, Editor), American Geophysical Union, Washington, D. C.

Johnson, J. C. (1954) Physical meteorology. Cambridge, Massachusetts: MIT Press, 393p.

Liljequist, G. (1957) Energy exchange of an Antarctic snowfield, Norwegian-British-Swedish Antarctic Expedition, 1949-52, Scientific Results, vol. II, part 1c, Oslo.

Mason, B. J. (1962) Clouds, rain and rainmaking. Cambridge, England: University Press.

Middleton, W. E. K. (1952) Vision through the atmosphere. Toronto: University of Toronto Press, 250p.

APPENDIX A: VISUAL RANGE DATA

Date 1964/65	Visual range km	Accumulation rate g cm^{-2} hr^{-1}	Fall vel. cm sec^{-1}	Snow density g m^{-3}	Snow type
Dec 4	1.2	0.104	134	0.216	0.4-mm crystals clustered into 1-mm groups and singly
4	1.4	0.195	140	0.387	0.4-mm crystals clustered into 1-mm groups and singly
6	7.2	0.00391	61	0.0178	Hexagonal "flowers" approx 1 mm diam
6	3.9	0.00618	61	0.0281	Hexagonal "flowers" approx 1 mm diam
15	2.7	0.00924	46	0.0558	Small flakes of stellar crystal < 1 mm diam
20	7.2	0.00308	70	0.0122	Flakes up to 1 cm diam consisting of stellar crystals 1 - 2 mm diam
20	1.1	0.0695	81	0.238	Flakes approx 1 cm diam with stellar crystals approx 2 mm diam
20	1.5	0.0283	81	0.097	Flakes approx 1 cm diam with stellar crystals approx 2 mm diam
22	3.2	0.0252	90	0.0778	0.6-mm rimed pellets
22	3.5	0.0284	80	0.0986	0.7-mm pellets and 1-mm "flowers"
22	2.9	0.0448	102	0.122	1-mm "flowers"
22	2.4	0.0522	78	0.186	Flakes approx 1 cm consisting of stellar crystals approx 1 mm
22	1.2	0.110	66	0.464	Flakes approx 1 cm consisting of stellar crystals approx 1 mm (slight wind)
Jan 13	3.0	0.0423	61	0.193	0.5-mm prisms and granules with some dendritic growth
13	2.6	0.0423	49	0.240	0.5-mm prisms and granules with some dendritic growth

APPENDIX A

Date 1965	Visual range km	Accumulation rate g cm^{-2} hr^{-1}	Fall vel. cm sec^{-1}	Snow density g m^{-3}	Snow type
Jan					
16	3.5	0.0311	71	0.122	0.3-mm diam spatial dendrites
16	2.15	0.0490	75	0.181	0.7-mm diam spatial dendrites
16	3.0	0.0277	91	0.0846	0.2-0.5-mm spatial dendrites
17	7.0	0.0048	61	0.0219	Flakes consisting of plane dendrites 4 mm diam
20	1.6	0.101	68	0.413	0.8-mm spatial dendrites
20	1.9	0.0589	81	0.202	Flakes approx 0.5-1.0 cm consisting of plane dendrites 2 mm
24	1.7	0.087	97	0.249	Fine needles, 2 mm long and 0.1 mm thick. Also 0.8-mm dendrites or perhaps cores of larger shattered stars, clumping into flakes
24	1.8	0.052	98	0.147	Clumped spicules, each 2 mm long, 0.1 mm thick
26	1.4	0.129	91	0.393	Flurrying flakes of 1-mm spatial dendrites
Feb					
5	4.5	0.0114	52	0.0609	0.2 mm diam, granular
5	3.8	0.0136	49	0.0771	0.1-0.7 mm diam, granular
10	2.0	0.269	122	0.611	2 mm long needles and ice granules clumping into flakes
18	3.4	0.0336	70	0.133	1-cm flakes consisting of approx 3 mm diam stellar dendrites
18	1.8	0.106	70	0.421	1-cm flakes consisting of approx 3 mm diam stellar dendrites
18	0.8	0.158	70	0.627	1-2 mm diam stars and flakes $\leq$ 1 cm diam
18	0.5	0.196	70	0.778	1-2 mm diam stars and flakes $\leq$ 1 cm diam
22	1.6	0.104	94	0.307	Flakes $\leq$ 1 cm diam consisting of spatial dendrites approx 2 mm

Date 1965	Visual range km	Accumulation rate g cm^{-2} hr^{-1}	Fall vel. cm sec^{-1}	Snow density g m^{-3}	Snow type
Feb					
22	1.2	0.107	73	0.407	Flakes ≤ 1 cm diam consisting of spatial dendrites approx 2 mm (slight turbulence)
26	1.3	0.118	98	0.333	Refrozen granules and flakes (evidence of prior melting)
26	1.1	0.153	106	0.401	Iced crystals approx 1 mm diam
Mar					
10	7.5	0.0056	76	0.0204	Fine granules and dendrites
20	7.0	0.00294	61	0.0134	0.5-mm spicules and approx 1-mm aggregations
20	4.6	0.00594	72	0.0229	Approx 2-mm aggregations of spicules and spatial dendrites
23	2.2	0.0251	81	0.086	Flakes > 1 cm consisting of stellar dendrites 4-5 mm diam
23	1.9	0.0288	87	0.092	Flakes > 1 cm of stellar dendrites approx 5 mm diam
23	3.6	0.0258	90	0.0796	Flakes approx 1 cm of stellar dendrites approx 4 mm diam
23	3.8	0.0166	81	0.0570	Flakes approx 1 cm and stars 4 mm diam
23	5.2	0.0125	84	0.0413	Flakes < 1 cm and stars 4 mm
23	6.5	0.0036	70	0.0143	1-mm spatial dendrites and 2-3-mm aggregations
23	2.2	0.0177	64	0.0768	Plane "flowers" and spicules ≤ 1 mm
23	3.4	0.0207	70	0.082	Plane "flowers" and spicules ≤ 1 mm
26	4.4	0.102	94	0.301	Flakes approx 1 cm ("warm")
26	4.6	0.0966	101	0.266	Rimed stars ≤ 5 mm
26	3.4	0.125	87	0.517	Rimed crystals and aggregations < 1 cm diam

APPENDIX A

Date 1965	Visual range km	Accumulation rate g cm^{-2} hr^{-1}	Fall vel. cm sec^{-1}	Snow density g m^{-3}	Snow type
Mar 26	2.2	0.150	122	0.341	Flakes $\geq$ 1 cm
29	0.8	0.138	81	0.472	Mainly 4 mm flakes with 1 mm spatial dendrites
29	3.0	0.0485	84	0.160	0.5 mm spatial dendrites, few small flakes
29	2.7	0.0945	87	0.302	1 mm rimed spatial dendrites
29	1.4	0.116	70	0.460	Rimed dendrites, 1-2 mm diam
29	1.1	0.175	74	0.657	Rimed dendrites, 1-2 mm diam, also capped columns
29	0.75	0.232	94	0.686	1-2mm diam dendrites

APPENDIX B: PARTICLE CONCENTRATION

Date 1965	Vertical flux cm^{-2} sec^{-1}	Fall velocity cm sec^{-1}	Concentration cm^{-3}	Density g m^{-3}	Snow type
Jan					
16	0.546	71	7.7×10^{-3}	0.122	0.3 mm spatial dendrites
16	1.40	91	15.4×10^{-3}	0.0846	0.2-0.5-mm spatial dendrites
20	0.656	68	9.64×10^{-3}	0.413	0.8-mm spatial dendrites
24	0.996	97	10.3×10^{-3}	0.249	Fine needles 2 mm long, 0.1 mm thick. Also 0.8-mm dendrites or fragments
24	0.586	98	5.97×10^{-3}	0.147	Clumped spicules, each 2 mm long, 0.1 mm thick
Feb					
5	0.396	52	7.62×10^{-3}	0.0609	0.2 mm diam grains
5	0.495	49	10.1×10^{-3}	0.0771	0.1-0.7 mm grains
20	0.156	61	2.56×10^{-3}	0.0134	0.5 mm spicules and 1-mm aggregations
20	0.363	72	5.04×10^{-3}	0.0229	2-mm aggregations of spicules and spatial dendrites
23	2×10^{-3}	87	2.30×10^{-5}	0.092	Flakes > 1 cm of stellar dendrites approx 5 mm
23	2×10^{-3}	81	2.47×10^{-5}	0.086	Flakes > 1 cm of plane dendrites 4-5 mm diam
26	5×10^{-3}	122	4.10×10^{-5}	0.341	Flakes > 1 cm of stellar dendrites
29	0.438	84	5.21×10^{-3}	0.160	0.5-mm spatial dendrites with few small flakes
29	0.581	87	6.68×10^{-3}	0.302	1-mm rimed spatial dendrites
29	0.476	70	6.80×10^{-3}	0.460	Rimed dendrites, 1-2 mm
29	0.371	74	5.01×10^{-3}	0.657	Rimed dendrites, 1-2 mm diam, and capped columns
29	1.18	94	12.5×10^{-3}	0.686	1-2-mm dendrites

APPENDIX C: ESTIMATED PARTICLE MASS

Snow type	Approximate mean particle mass (g)
0.3 mm diam spatial dendrite	1.47×10^{-5}
0.2-0.5 mm diam spatial dendrite	5.5×10^{-6}
0.8 mm diam spatial dendrite	4.29×10^{-5}
0.2 mm rimed grains	7.99×10^{-6}
0.1-0.7-mm rimed grains	7.63×10^{-6}
0.5 mm diam spatial dendrites	3.07×10^{-5}
1-mm rimed spatial dendrites	4.52×10^{-5}
1-2-mm rimed plane dendrites	5.49×10^{-5}
1 mm diam hexagonal "flowers" (plane dendrites with plates on arms)	2×10^{-6}
1-mm stellar dendrites	1.5×10^{-6}
1-2 mm diam stellar dendrites	5×10^{-6}
Needles, 2 mm long, 0.1 mm thick	1.4×10^{-5}

14. KEY WORDS	LINK A		LINK B		LINK C	
	ROLE	WT	ROLE	WT	ROLE	WT
Snow precipitation--Optical effects Snow precipitation--Reflective properties Snow crystals--Coalescence Visibility--Meteorological factors						

INSTRUCTIONS

1. ORIGINATING ACTIVITY: Enter the name and address of the contractor, subcontractor, grantee, Department of Defense activity or other organization *(corporate author)* issuing the report.

2*a*. REPORT SECURITY CLASSIFICATION: Enter the overall security classification of the report. Indicate whether "Restricted Data" is included. Marking is to be in accordance with appropriate security regulations.

2*b*. GROUP: Automatic downgrading is specified in DoD Directive 5200.10 and Armed Forces Industrial Manual. Enter the group number. Also, when applicable, show that optional markings have been used for Group 3 and Group 4 as authorized.

3. REPORT TITLE: Enter the complete report title in all capital letters. Titles in all cases should be unclassified. If a meaningful title cannot be selected without classification, show title classification in all capitals in parenthesis immediately following the title.

4. DESCRIPTIVE NOTES: If appropriate, enter the type of report, e.g., interim, progress, summary, annual, or final. Give the inclusive dates when a specific reporting period is covered.

5. AUTHOR(S): Enter the name(s) of author(s) as shown on or in the report. Enter last name, first name, middle initial. If military, show rank and branch of service. The name of the principal author is an absolute minimum requirement.

6. REPORT DATE: Enter the date of the report as day, month, year; or month, year. If more than one date appears on the report, use date of publication.

7*a*. TOTAL NUMBER OF PAGES: The total page count should follow normal pagination procedures, i.e., enter the number of pages containing information.

7*b*. NUMBER OF REFERENCES: Enter the total number of references cited in the report.

8*a*. CONTRACT OR GRANT NUMBER: If appropriate, enter the applicable number of the contract or grant under which the report was written.

8*b*, 8*c*, & 8*d*. PROJECT NUMBER: Enter the appropriate military department identification, such as project number, subproject number, system numbers, task number, etc.

9*a*. ORIGINATOR'S REPORT NUMBER(S): Enter the official report number by which the document will be identified and controlled by the originating activity. This number must be unique to this report.

9*b*. OTHER REPORT NUMBER(S): If the report has been assigned any other report numbers *(either by the originator or by the sponsor)*, also enter this number(s).

10. AVAILABILITY/LIMITATION NOTICES: Enter any limitations on further dissemination of the report, other than those imposed by security classification, using standard statements such as:

(1) "Qualified requesters may obtain copies of this report from DDC."

(2) "Foreign announcement and dissemination of this report by DDC is not authorized."

(3) "U. S. Government agencies may obtain copies of this report directly from DDC. Other qualified DDC users shall request through _____."

(4) "U. S. military agencies may obtain copies of this report directly from DDC. Other qualified users shall request through _____."

(5) "All distribution of this report is controlled. Qualified DDC users shall request through _____."

If the report has been furnished to the Office of Technical Services, Department of Commerce, for sale to the public, indicate this fact and enter the price, if known.

11. SUPPLEMENTARY NOTES: Use for additional explanatory notes.

12. SPONSORING MILITARY ACTIVITY: Enter the name of the departmental project office or laboratory sponsoring *(paying for)* the research and development. Include address.

13. ABSTRACT: Enter an abstract giving a brief and factual summary of the document indicative of the report, even though it may also appear elsewhere in the body of the technical report. If additional space is required, a continuation sheet shall be attached.

It is highly desirable that the abstract of classified reports be unclassified. Each paragraph of the abstract shall end with an indication of the military security classification of the information in the paragraph, represented as *(TS)*, *(S)*, *(C)*, *or (U)*.

There is no limitation on the length of the abstract. However, the suggested length is from 150 to 225 words.

14. KEY WORDS: Key words are technically meaningful terms or short phrases that characterize a report and may be used as index entries for cataloging the report. Key words must be selected so that no security classification is required. Identifiers, such as equipment model designation, trade name, military project code name, geographic location, may be used as key words but will be followed by an indication of technical context. The assignment of links, rules, and weights is optional.

Unclassified
Security Classification

DOCUMENT CONTROL DATA - R&D

(Security classification of title, body of abstract and indexing annotation must be entered when the overall report is classified)

1. ORIGINATING ACTIVITY *(Corporate author)*
U.S. Army Cold Regions Research and Engineering Laboratory, Hanover, N. H.

2a. REPORT SECURITY CLASSIFICATION
Unclassified

2b. GROUP

3. REPORT TITLE
LIGHT SCATTERING AND PARTICLE AGGREGATION IN SNOWSTORMS

4. DESCRIPTIVE NOTES *(Type of report and inclusive dates)*
Research Report

5. AUTHOR(S) *(Last name, first name, initial)*
Mellor, Malcolm

6. REPORT DATE	7a. TOTAL NO. OF PAGES	7b. NO. OF REFS
Feb 1966	20	5

8a. CONTRACT OR GRANT NO.

b. PROJECT NO.

c. DA Task IV025001A13001

d.

9a. ORIGINATOR'S REPORT NUMBER(S)
Research Report 193

9b. OTHER REPORT NO(S) *(Any other numbers that may be assigned this report)*

10. AVAILABILITY/LIMITATION NOTICES
Distribution of this document is unlimited

11. SUPPLEMENTARY NOTES

12. SPONSORING MILITARY ACTIVITY
U.S. Army Cold Regions Research and Engineering Laboratory

13. ABSTRACT

Attenuation of visible radiation by falling snow was studied by a method based on brightness contrast between topographic features and the adjacent sky. Extinction coefficient and visual range are related to snow density, and are compared with data for Antarctic blizzards. Since attenuation depends more on the size and concentration of discrete particles than on the mass density of suspended snow, the process of particle aggregation and snowflake formation during fall is considered by collision theory, and an expression describing aggregation effects is developed. This offers an explanation for the relative constancy of particle concentration observed at ground level during snowfalls of varying density. Since there is no strong justification for relating extinction coefficient to snow density, an empirical correlation between extinction coefficient and precipitation rate is given for practical use. It is shown that visual range estimated by eye in hilly terrain may be less than the true value, since sky-brightness is locally reduced over broad hilltops with low albedo.

DD FORM 1 JAN 64 1473

Unclassified
Security Classification